

Artificial Landmark Design and Detection Using Hierarchy Information for UAV Localization and Landing

Wen Fei¹, Zhuo Su^{*1}, Changfu Zhou¹

1. Northeastern University, Shenyang, 110819, China
E-mail: neu_suzhuo@qq.com

Abstract: Localization and landing are of fundamental importance for Unmanned Aerial Vehicles (UAVs), and with the research on compute vision information processing, artificial landmark detection, a more efficient and accurate method, becomes a hot topic. In this paper, in order to provide sufficient information for localization, we design an artificial landmark with an annulus and some circles inside with specific positions and colors. We firstly use color and hierarchy information to find possible pattern, then calculate its cross-ratio to check this pattern, localize our UAV at last.

To prove our landmark and detection-recognition algorithm, two kinds of experiments are conducted and the results demonstrate our feasibility and accuracy. One is putting our landmark on random backgrounds to imitate complex environment, another is on real environments with different projection and distance. With those experimental results, we get the conclusion that our landmark and algorithm are robust and feasibility under various environments.

Key Words: UAV, artificial landmark, multiple feature, hierarchy information, cross-ratio

1 Introduction

With the development of Unmanned Aerial Vehicles (UAVs), accurately identifying landmark, landing on mobile platforms (such as ships, large vehicles) and narrow areas (such as city, factory) environments have a wide range of applications now. Based on inertia component, sound, microwave, and GPS, UAVs currently can achieve localization and navigation, but still cannot meet the accuracy requirement for precise landing: errors of inertia navigation system will accumulate with time and lead a poor precision for long term; acoustic navigation technology is easily interfered by noise; microwave navigation method cost high, and raises great requirements for UAVs, while civil GPS satellite navigation precision only reaches 1 meters. In contrast, visual navigation with small size equipment can get high accurate, informative results. The application of visual technology for precise localization of UAVs is of great significance for researchers.

Landmarks for navigation system can be divided into artificial landmarks and natural landmarks. As for natural landmarks, often with the learning process and strong adaptability, can easily be applied to a variety of occasions, F.Mirus and his coworkers [1] proposed a method for feature extraction from natural landmarks, achieving satisfying localization under certain conditions. However, natural landmark detection systems require strong capability in data processing, which is rarely applied to tintype UAVs. Compared with natural landmarks, using artificial landmark system with relatively simple processing to acquire accurate position in a complex environment is a more effective way for the UAVs landing.

Artificial landmarks are mostly used to provide navigation information for mobile robots. Guo Yang [2] designed the landmarks composed of the symmetric rectangle and

seven-segment digital, using symmetric structure and specific colors for determining interest areas, digital pattern for specific information of location, to guide the robot forward. The symmetric repetition structure of the landmark proposed by Kuk-Jin Yoon et al. [3] that can adapt to variable illumination and distance, using recursive way to search interest area, to some extent, this method can improve the detection efficiency. Huletski et al. [4] made an artificial landmark similar to QR code, depending on the colors to identify interest area as well. Zhang Guangjun [5], who proposed a landmark pattern with double circle, detected the cross ratio, an invariant of projection, constructed on this pattern, thereby solves UAV's position. Li Yu and his team [6] made use of affine invariant moment and support vector machine to test combination six-round landmark, which still works in the case of partial deletion of the landmark. However, Jayatilleke [7] verified application of pattern recognition in UAV landmark detection and showed its lack of high requirements for image quality.

Designs and applications of these landmarks are mainly based on a single detecting method, mostly color detection and cross ratio invariance, which generally meets the needs of mobile robot localization. However, environment of UAVs is more complex, with stronger image noise. We need to extract more information from the landmark and improve anti-interference ability of detection algorithms. Then, a landmark with features of color, outline hierarchy and geometric invariants (cross ratio), as well as an effective detection and localization algorithm are proposed.

2 Landmark design of unmanned aerial vehicle

To design the landmark, a basic requirement is to contain the easily distinguishable information, which is the key to feature extraction. Besides, the information should be extracted easily, which can be measured as relative size of feature pattern. Of course, we expect to extract the

corresponding feature information even in the condition of low image resolution. On the other hand, the characteristic pattern should have strong anti-interference ability. Environmental disturbances are generally divided into two situations, false-detecting namely the external environment having the characteristics of the landmark, resulting in miscarriage of justice; leaking-detecting, the environmental having destroyed the image features leading to the miscarriage of justice. And for UAV landing system, the latter has a more serious impact.

Central projection does not change either color information or contour information of the landmark but destroys the symmetry of the object. Therefore, we mainly take advantage of the color and contour information to recognize the landmark. Because cross ratio is an important invariant of central projection [8], we then screen possible pattern to decrease error caused by false-detecting. Considering that the position of UAV is difficult to determine, we take the circle as the basic element in this paper. The four solid circles are asymmetrically placed within the ring because the single circular cannot provide orientation information.

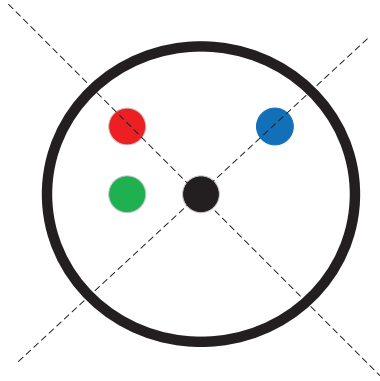


Fig.1 The landmark with multi-feature

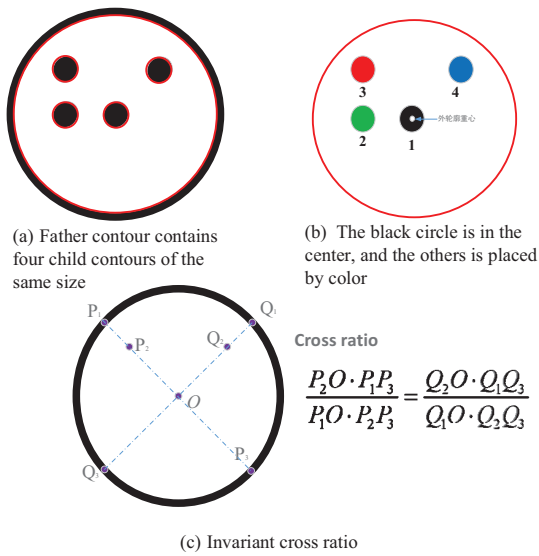


Fig.2 Analysis of landmark features

In this paper, we utilize color feature to place the inner solid circles as shown in Fig.1, of which the black one is in the center, and the periphery is placed by the solid circles of

three colors, red, green and blue. Besides, these circles are identified and the feature is analyzed as shown in Fig.2.

3 Landmark recognition and feature extraction

In this paper, the basic element of landmark design is the circle, and the feature points to be extracted are its center, so the characteristic of circles under projection is very pivotal.

3.1 Analysis of circular central projection mode

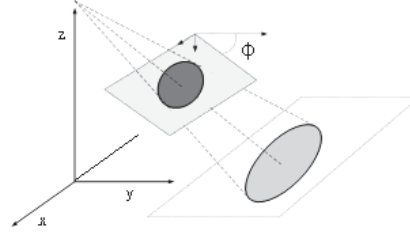


Fig.3 A circle under central projection

For the projection model shown in Fig.3, the circle in the landmark plane is marked as C , with three-dimensional coordinate $(x, y, 0)$, so the landmark curve is:

$$O_1 + a \cdot C \quad (1)$$

With rotation angle φ , we get:

$$[O_1 + a \cdot C] \begin{bmatrix} 1 & 0 & 0 \\ 0 & \cos \varphi & \sin \varphi \\ 0 & -\sin \varphi & \cos \varphi \end{bmatrix} \quad (2)$$

So, the resulted curve on the projection plane is:

$$\begin{bmatrix} x' \\ y' \\ 1 \end{bmatrix} = \frac{1}{z_c} \begin{bmatrix} f & 0 & 0 \\ 0 & f & 0 \\ 0 & 0 & 1 \end{bmatrix} [O_1 + a \cdot C] \begin{bmatrix} 1 & 0 & 0 \\ 0 & \cos \varphi & \sin \varphi \\ 0 & -\sin \varphi & \cos \varphi \end{bmatrix} \quad (3)$$

$$O_1(0, y_0, z_0)$$

$$C : (x, y, 0) \quad x^2 + y^2 = 1$$

Here, (x', y') is the point on the projective plane, and the curve on the projection plane is not ellipse, that is to say, the center of the circle is not an invariant of central projection.

But when $y_0 \ll z_0$, $[O_1 + a \cdot C]$ can be simplified as (x, y, z_0) . The curve corresponds to the result of affine transformation, and the set of projection points forms an ellipse, which will be used in test experiment for landmark detection algorithm.

3.2 Image processing

For the possible landmark that is shown in Fig. 4 (a), we first find out all the outer contours and get the outer ring as shown in Fig. 4 (b). Then, we extract the four sub contours inside the ring, which makes use of the hierarchical information of contours to find landmark, as shown in Fig. 4 (c). In order to recognize landmarks further, in this paper, we check up the color feature of inner solid circle, which avoids miscarriage of justice. And at the same time, this paper sorts the four feature points in the interior as shown in

Fig. 4 (d). The straight line passing through point 1 and point 3 intersects with the outer contour at point 6 and point 8, and the straight line passing through point 1 and point 4 intersects with the outer contour at point 5 and point 7, if the cross ratios of the two straight lines are the same, the landmark has been found correctly.

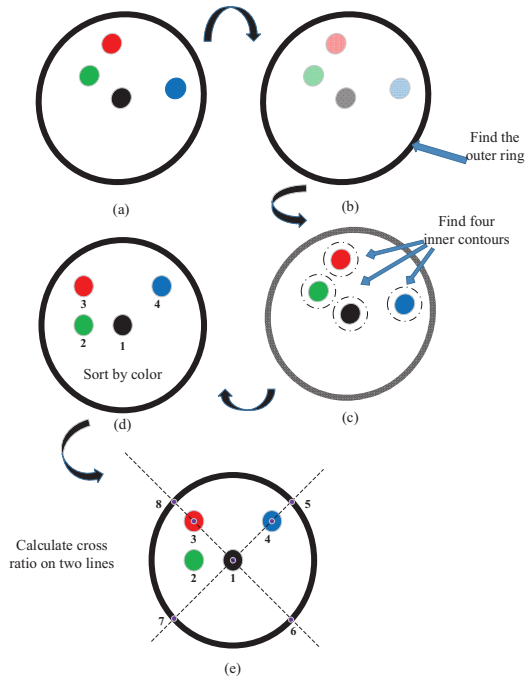


Fig.4 Diagram of imaging processing

3.3 Landmark detection algorithm

The program of landmark detection algorithm is written on the base of OpenCV, and the flowchart of algorithm is shown in Fig. 5, which is generally divided into binarization, checking both contour and color features and verification of cross ratio.

In the process of binary image's generation, the program uses different methods for images with different resolution. There is an edge detection algorithm *canny* [9] for high resolution images, it uses convolution array to obtain two-dimensional gradient, where the value of theta is an integer multiple of 45 degrees.

$$\frac{\partial}{\partial x} = G_x = \begin{bmatrix} -1 & 0 & 1 \\ -2 & 0 & 2 \\ -1 & 0 & 1 \end{bmatrix} \quad \frac{\partial}{\partial y} = G_y = \begin{bmatrix} -1 & -2 & -1 \\ 0 & 0 & 0 \\ 1 & 2 & 1 \end{bmatrix} \quad (4)$$

$$G = \sqrt{G_x^2 + G_y^2} \quad \theta = \arctan\left(\frac{G_x}{G_y}\right)$$

However, for images with low resolution, the edge is not obvious, where a user-defined threshold method is needed. The average value of the area is obtained by using $(2n+1) \times (2n+1)$ Gauss or mean matrix, and then compared with the central pixel. Since the landmark belongs to the feature with low color component, the paper set the constant C as 5.

$$f_{mean} = \sum_{i,j=-n}^n f_{i,j} \cdot p_{i,j} - C \quad (5)$$

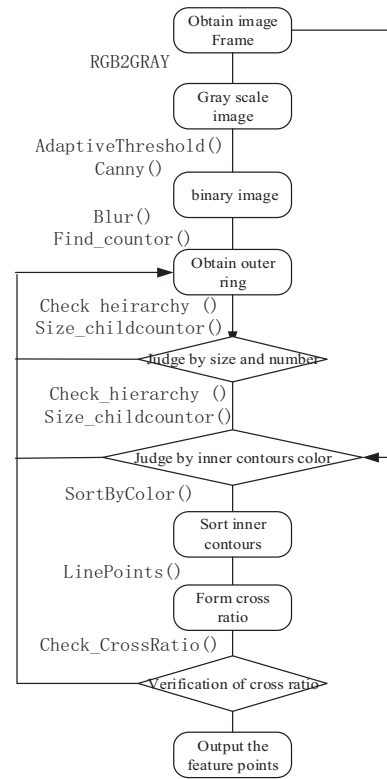


Fig.5 Flowchart of processing algorithm

Gauss matrix 5*5 is:
$$P_{Gauss,n} = \begin{bmatrix} 1 & 2 & 3 & 2 & 1 \\ 2 & 5 & 6 & 5 & 2 \\ 3 & 6 & 8 & 6 & 3 \\ 2 & 5 & 6 & 5 & 2 \\ 1 & 2 & 3 & 2 & 1 \end{bmatrix}$$

Comparing $f_{mean}(x, y)$ with $f(x, y)$:

$$f_{binary}(x, y) = \begin{cases} 0 & f_{mean}(x, y) > f(x, y) \\ 255 & f_{mean}(x, y) < f(x, y) \end{cases} \quad (6)$$

Here, $f_{binary}(x, y)$ is the pixel value of this point, and then it deepens image edge through fuzzification.

After the actual debugging, the efficiency of the detection algorithm in the computer with frequency of 2.0Ghz and 8GB memory can be stabilized at 40 frame /s, which can meet real-time image processing requirements for UAVs.

4 Pose estimation based on this landmark

Despite a variety of image acquisition equipment, we use single ordinary CCD camera in this paper.

Firstly, we introduce the concept of image physical coordinate frame to deduce transformation of the image coordinate and UAV-based coordinate frame. It is defined as the UAV-based frame's origin moving to the center of the focal plane. The image physical coordinate frame is transformed into the image coordinate when described as the pixel point.

Relationship between image physical coordinate frame and UAV-based frame:

$$\begin{bmatrix} u \\ v \\ 1 \end{bmatrix} = \begin{bmatrix} \frac{1}{dx} & 0 & u_0 \\ 0 & \frac{1}{dy} & v_0 \\ 0 & 0 & 1 \end{bmatrix} \begin{bmatrix} u' \\ v' \\ 1 \end{bmatrix} \quad (7)$$

Relationship between image physical coordinate frame and image coordinate:

$$\begin{bmatrix} u' \\ v' \\ 1 \end{bmatrix} = \frac{1}{z'} \begin{bmatrix} f & 0 & 0 \\ 0 & f & 0 \\ 0 & 0 & 1 \end{bmatrix} \begin{bmatrix} x' \\ y' \\ z' \end{bmatrix} \quad (8)$$

Combine two equations above:

$$\begin{bmatrix} u \\ v \\ 1 \end{bmatrix} = \frac{1}{z'} \begin{bmatrix} a_x & 0 & u_0 \\ 0 & a_y & v_0 \\ 0 & 0 & 1 \end{bmatrix} \begin{bmatrix} x' \\ y' \\ z' \end{bmatrix} \quad (9)$$

Among which, $\begin{bmatrix} u \\ v \\ 1 \end{bmatrix}$ represents point on image plane,

located on focal plane as $\begin{bmatrix} x' \\ y' \\ z' \end{bmatrix}$ with focal length f . We

simplify as $\mathbf{v} = \mathbf{M}\xi' / \xi'_3$, which indicates the relation of $\mathbf{v} \Leftrightarrow \xi'$, \mathbf{v} in image plane, ξ' is the position on UVA-based frame.

Relation between UAV-based frame and World frame is:

$$\begin{bmatrix} x' \\ y' \\ z' \end{bmatrix} = \mathbf{R} \begin{bmatrix} x \\ y \\ z \end{bmatrix} + \mathbf{T} = \begin{bmatrix} r_{11} & r_{12} & r_{13} \\ r_{21} & r_{22} & r_{23} \\ r_{31} & r_{32} & r_{33} \end{bmatrix} \begin{bmatrix} x \\ y \\ z \end{bmatrix} + \begin{bmatrix} t_x \\ t_y \\ t_z \end{bmatrix} \quad (10)$$

Among which, $\begin{bmatrix} x' \\ y' \\ z' \end{bmatrix}$ and $\begin{bmatrix} x \\ y \\ z \end{bmatrix}$ are respectively coordinate on

UAV-based frame and World frame. When using rotation matrix \mathbf{R} as function of UAV posture, World frame coordinate \mathbf{T} , we write as $\xi' = \mathbf{R}\xi + \mathbf{T}$.

Considering all equations above, we get:

$$\xi'(3) = \mathbf{R}(:, 3)\xi + \mathbf{T}(3) \quad (11)$$

Combining with equations (9), (10):

$$\begin{cases} \xi' = \mathbf{R}\xi + \mathbf{T} \\ \mathbf{v} = \mathbf{M}\xi' / \xi'_3 \end{cases} \Rightarrow \mathbf{v} = \mathbf{M}(\mathbf{R}\xi + \mathbf{T}) / (\mathbf{R}(:, 3)\xi + \mathbf{T}(3)) \quad (12)$$

Analyzing the equation, we need to solve 10 variables in parameters \mathbf{M} , \mathbf{R} , \mathbf{T} . However, u_0 , v_0 are basically half of the size of image. Thereby, we need 4 nonlinear points to calculate 8 parameters [10].

To get high accuracy, it's supposed to consider distortion of camera and calibrate camera parameters [11] [12]. After calibration, we get the values of a_x and a_y , and only need three points to solve the equations.

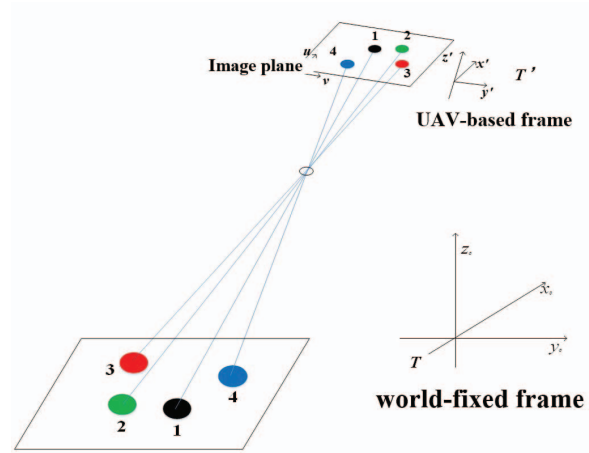


Fig.6 Transformation between coordinate frames

As shown in Fig. 6, relation between the different coordinates will be used to localization combining with features in landmark.

5 Experimental data and analysis

In order to test the reliability of landmark recognition in various complex environments, this paper makes a complex background test firstly. Test uses the program to detect the landmark that placed in the different backgrounds after affine transformation. (The center projection can be simulated by affine transformation when the distance is far.) In this paper, 500 background images are selected randomly, and the recognition rate is as high as 97%, which fully proves the adaptability of the landmark designed in this paper to the complex environment. Examples of complex background experiment are shown in Fig.7.



Fig.7 Simulation of complex environments

In the actual environment, there are many factors that make it difficult to distinguish meanwhile, such as uneven illumination distribution and distortion of the image caused by different visual angle. In this paper, experiments are also carried out on the actual environment.

Fig. 8 shows the actual state of landmark detection. Due to the limitation of resolution, there are only four to five pixels on these solid circle contours, besides when the inclined visual angle has reached 40 degrees, the landmark detection becomes more difficult. However, the detection on this

paper can still accurately find the feature points, and fix a position.

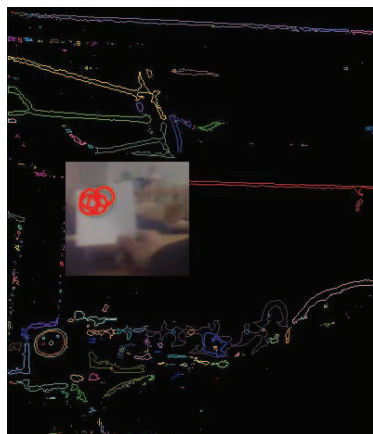


Fig.8 Landmark detection

In order to test the influence of landmark design on positioning, the quad-rotor UAV helicopter is equipped with a FOV camera whose optical part is made of 20mm lens in this paper. In the experiment, the video data and the position data are collected firstly, and then the image frame of the 1280*720 pixels is reduced to 600*340 pixels and sent to the detection system for localization. By the way, the size of the landmark is 1.5*1.0 m², which is in line with the actual situation.

This paper focuses on the test of the relationship between the positioning error and height. The experiment sets different flight height, and the UAV within the angle of 30degrees flies around the landmark at a low speed, and collects image information of 100 frames at each height. Position data after calculation and processing is compared with real time height of UAV as shown in Fig.9, in which the orange curve represents the number of detected image frames and the blue one represents the estimate error. It can be seen that the landmark of this paper is quite effective within the height of 7m. However, when the image information collected between 7~8m is analyzed, it is found that the width of the landmark is only 20 pixels. In this case, there is a serious rupture of the contour and the feature information is difficult to extract effectively. Fig.10 shows the experimental results of the height above 3m, it can be seen that the landmark has been accurately identified.

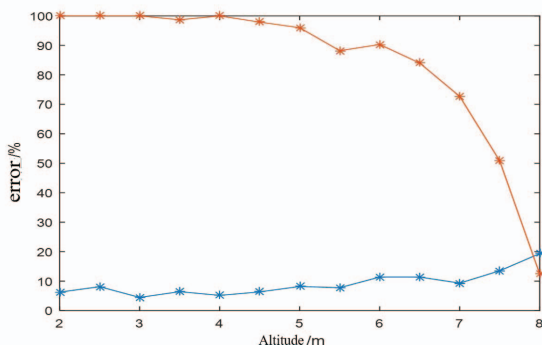


Fig.9 Detection error vs. altitude (orange curve for detection rate, blue one for estimate error)

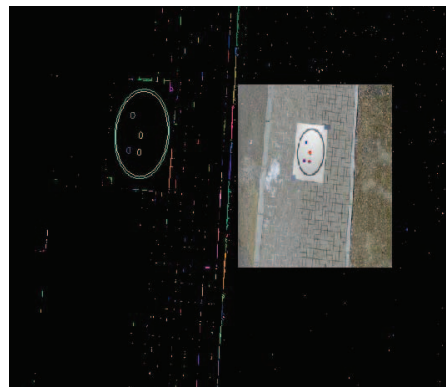


Fig.10 Detection at 3m height

On the basis of the above experiments, we do an experimental study on the indoor precise landing of a quad-rotor UAV helicopter. Parrot AR.Drone 2.0 is selected as the experimental vehicle. As for the testing environment, it is a corridor of laboratory which is 5 meters wide, and the landmark is placed 8 meters ahead of the UAV. As shown in Fig.11, AR.drone flies forward after taking off, and transfers real-time image data back to the computer meanwhile. Then the computer processes image data and calculates pose information to give UAV a flight command or a landing instruction. A large number of experiments have proved that the UAV can accurately land within the range of 10cm around the landmark through the landmark and detection algorithm in this paper.

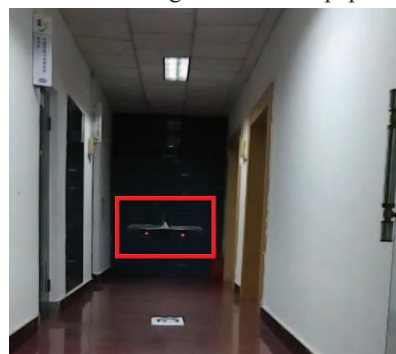


Fig.11 Experiment of auto-landing for UAV

6 Conclusion

In this paper, real-time video image processing based on our multi-feature artificial landmark and corresponding detection algorithm realizes localization of Unmanned Aerial Vehicles and assists accurate landing. Through our experience and theoretical analysis, the landmark and detection algorithm are applicable for various environments, which give effective support to drone objects like UAVs.

Acknowledgment

This work was partly supported by National Natural Science Foundation of China (No.61471110), Foundation of Liaoning Educational Department(L2014090), and Chinese Universities Scientific Foundation (N16261004- 2/3/5).

References

- [1] Mirus, Florian, et al. "A modular hybrid localization approach for mobile robots combining local grid maps and natural landmarks." *ACM Symposium on Applied Computing ACM*, 2016:287-290.
- [2] Guo, Yang, and X. Xu. "Landmark Design Using Projective Invariant for Mobile Robot Localization." *IEEE International Conference on Robotics and Biomimetics, Robio 2006, Kunming, China, 17-20 December 2006*:852-857.
- [3] Yoon, Kuk Jin, and I. S. Kweon. "Landmark design and real-time landmark tracking for mobile robot localization." *Proceedings of SPIE - The International Society for Optical Engineering* 4573.20(2002):219-226.
- [4] Huletski, A., D. Kartashov, and K. Krinkin. "The artificial landmark design for mobile robots localization and mapping." (2015):56-61.
- [5] Guangjun Zhang, Fuqiang Zhou "Based on double characteristic of UAV landing position and attitude measurement method" *Chinese Journal of Aeronautics* 26.3(2005):344-348.
- [6] Yu Li et al. "Vision-based autonomous landing of UAV landmark recognition." *Computer application research* 29.7(2012):2780-2783.
- [7] Jayatilleke, Lalindra, and N. Zhang. "Landmark-based localization for Unmanned Aerial Vehicles." *Systems Conference* 2013:448 - 451.
- [8] Faugeras, Olivier. "Stratification of three dimensional vision: projective, affine, and metric representations: errata." *Journal of the Optical Society of America A* 12.7(1995):1606-1606.
- [9] Xingyun Mao, Xuefei Leng, Binghui Wang, *OpenCV3 introduction to programming*. Publishing House of electronics industry.
- [10] Zhang, Zhengyou. "A Flexible New Technique for Camera Calibration." *IEEE Transactions on Pattern Analysis & Machine Intelligence* 22.11(2000):1330-1334.
- [11] Jianfeng Dai. *Automatic calibration system for camera radial distortion*. South China University of technology, 2010.
- [12] Changyuan Wang, Jing Hou. "Improved method of camera calibration based on OpenCV" *Computers and digital engineering*, 42.1 (2014): 138-141.